International Journal of Radiation Oncology biology • physics

www.redjournal.org

Biology Contribution

Therapeutic Effects of Human Umbilical Cord–Derived Mesenchymal Stem Cells on Canine Radiation-Induced Lung Injury

Yuhui Hao, PhD,* Yonghong Ran, MS,* Binghui Lu, PhD,* Jiayin Li, PhD,† Jiaojiao Zhang, PhD,† Chunjing Feng, PhD,‡ Jinhui Fang, PhD,† Ruoyu Ma, PhD,† Zhihui Qiao, MS,§ Xiaotian Dai, MD,§ Wei Xiong, MD,§ Jing Liu, MS,* Qi Zhou, PhD,‡ Jie Hao, PhD,‡ Rong Li, PhD,* and Jianwu Dai, PhD*,†

State Key Laboratory of Trauma, Burns and Combined Injury, Institute of Combined Injury, Chongqing Engineering Research Center for Nanomedicine, College of Preventive Medicine, Third Military Medical University, Chongqing, China; †State Key Laboratory of Molecular Developmental Biology, Institute of Genetics and Developmental Biology, Chinese Academy of Sciences, Beijing, China; ‡Institute of Animals, Chinese Academy of Sciences, Beijing, China; and §Department of Respiratory Diseases, Southwest Hospital, Third Military Medical University, Chongqing, China

Received Jan 21, 2018, and in revised form May 2, 2018. Accepted for publication May 25, 2018.

Summary

Radiation-induced lung injury is a common complication after radiation therapy for thoracic tumors. Our studies show that canine radiation-induced lung injury could be observed at 180 days after x-ray radiation at 15 Gy, and intratracheal transplantation of mesenchymal stem cells can reduce oxidative stress,

Purpose: To investigate the effect of human umbilical cord–derived mesenchymal stem cell (MSC) transplantation on canine radiation-induced lung injury.

Methods and Materials: Beagle dogs received localized 15-Gy x-ray radiation to the right lower lung to establish the model of radiation-induced lung injury. After 180 days, dogs were divided into 2 groups (4 per group). The MSC group received intratracheal MSC transplantation, and the saline group received the same volume of normal saline by lavage. The effect of MSC transplantation on lung injury was then evaluated 180 days after transplantation.

Results: At 180 days after 15-Gy radiation, canine arterial blood oxygen partial pressure was significantly decreased, and the levels of hydroxyproline and transforming growth factor (TGF)-β in peripheral blood were significantly increased, whereas that of TGF-α was significantly decreased. Computed tomography evaluation revealed visible honeycomb shadows in the right middle and lower pulmonary pleurae. Blood

Reprint requests to: Rong Li, PhD, Third Military Medical University, Institute of Combined Injury State Key Laboratory of Trauma, Burns and Combined Injury, Chongqing, Engineering Research Center for Nanomedicine, College of Preventive Medicine, No 30 Gaotanyan St, Shapingba District, Chongqing 400038, China. Tel: +86 23 68752281; E-mail: yuhui_hao@126.com

This work was supported by the Science Foundation of the Chinese Academy of Sciences (grant no. XDA01030501), the National Natural Science Fund (grant nos. 81472913 and 81741112), the Chongqing Science Fund (grant no. cstc2016jcyjA0408), and the State Key Laboratory of Trauma, Burns and Combined Injury in China (grant no. SKLZZ201503).

Conflict of interest: none.

Supplementary material for this article can be found online at www.redjournal.org.

Int J Radiation Oncol Biol Phys, Vol. 102, No. 2, pp. 407–416, 2018
0360-3016/$ - see front matter
https://doi.org/10.1016/j.ijrobp.2018.05.068

inflammatory reactions, and transforming growth factor-β−Smad2/3 pathway activation, thereby reducing lung injury. This finding provides a basis for the application of mesenchymal stem cells in clinical transplantation therapies for radiation-induced lung injury.

oxygen partial pressure of the MSC group gradually increased over time, whereas the levels of hydroxyproline and TGF-β in the peripheral blood showed a decreasing trend; TGF-α levels gradually increased, which differed significantly from the results observed in the saline group. In addition, computed tomography and pathologic examination showed that the degree of lung injury in the MSC group was milder. The MSC group also showed significantly increased pulmonary superoxide dismutase levels and significantly decreased tumor necrosis factor-α, Interleukein-1, and hyaluronic acid levels. Further study confirmed that MSC transplantation inhibited the activation of TGF-β−Smad2/3 in lung tissues, and in vitro experiments showed that medium conditioned with MSCs effectively inhibited the increase in Smad2 and 3 levels induced by TGF-β1.

Conclusion: Canine radiation-induced lung injury could be observed at 180 days after radiation at 15 Gy. MSC transplantation can reduce oxidative stress, inflammatory reactions, and TGF-β−Smad2/3 pathway activation, thereby reducing lung injury.

Introduction

Radiation-induced lung injury is a common complication after total body radiation or radiation therapy for thoracic tumors and includes radiation pneumonitis in the early stage and radiation-induced pulmonary fibrosis (PF) in late stages (1-3). Radiation pneumonitis usually occurs in the first 6 to 12 weeks after thoracic radiation therapy, and PF occurs approximately 6 to 24 months after radiation (4, 5). Radiation-induced lung injury is a major obstacle affecting the success rate of thoracic tumor radiation therapy. Active exploration of treatment strategies to suppress lung injury is imperative (6).

Despite a number of potential treatments, such as methods targeting inflammatory cytokines, epithelial-mesenchymal transformation, the transforming growth factor-β (TGF-β) pathway, and senescent type II pneumocytes, PF still has a poor prognosis and a high mortality rate (7-9). Mesenchymal stem cells (MSCs) have pluripotent differentiation abilities, immunomodulatory functions, and paracrine characteristics and have brought hope for the treatment of radiation-induced PF (10). Many studies have confirmed that MSCs can promote alveolar epithelial cell repair and reduce inflammatory damage, fibroblast growth, and lung collagen deposition (11-15). MSCs also have significant immunosuppressive abilities and low immunoreactivity and therefore have advantageous safety features in autograft or allograft disease treatment (16). MSC transplantation inhibited radiation-induced lung injury in mice and reduced the risk of lung metastasis (17).

However, only a limited number of clinical and preclinical studies have been published on stem cell therapy for radiation-induced lung injury, especially for radiation-induced PF (18). In addition, only a small number of ongoing clinical trials have investigated idiopathic PF (19). The low engraftment rate and poor survival rate of MSC would influence therapeutic benefit. Current studies mostly use rats, mice, and other animal models, and few studies have used large-animal models. To determine whether MSC have a therapeutic effect on radiation-induced lung injury in large animals, this study established a lung injury model via local x-ray radiation of the right lower lung in dogs and evaluated the effect of intratracheal MSC transplantation. We also explored the potential protective mechanism of MSCs.

Materials and Methods

Animals

Male beagle dogs were used, as described in Materials E1 (available at www.redjournal.org). The experiments were approved by the Animal Ethics Committee of the Third Military Medical University and the Institutional Review Board.

Radiation

The 8 dogs were exposed to a single dose of 15 Gy radiation of right lower lung (Fig. E1 and Materials E1; available online at www.redjournal.org). The 15-Gy radiation dose was based on previous related experimental studies (17, 20).

Isolation and culture of human umbilical cord MSCs

Isolation and culture of MSCs from human newborn umbilical cord tissues were conducted according to our preliminary study (21, 22) (Materials E1; available online at www.redjournal.org). Consent to use the umbilical cords was obtained from the parents and families of the newborns, and the study was approved by the Animal Ethics Committee of the Third Military Medical University.

Intratracheal transplantation of MSCs

At 180 days after radiation, 8 dogs were randomly divided into 2 groups (4 per group): the saline group and the MSC group. To avoid clumping, MSCs were harvested with 0.25% trypsin/1 mM EDTA and washed with phosphate-buffered saline. After anesthesia, MSC transplantation (1×10^6 cells/kg) or normal saline lavage was conducted via bronchofiberscopy. The procedure was performed close to the lower right lung in a volume of 20 mL. No mortality was associated with the transplantation procedure. The single dose of MSC was chosen on the basis of the mean body mass and was equivalent to the effective dose used in relevant studies (23). At 180 days after transplantation, the dogs were sacrificed, and the lung tissues and serum samples were used for related examination.

Chest computed tomography examination

At 180 days after radiation, the dogs underwent computed tomography of the chest under full anesthesia by using a third-generation computed tomography (CT) scanner (SOMATOM Definition, Siemens, Forchheim, Germany). The CT scan was performed again at 3 days, 30 days, 90 days, and 180 days after the dogs received a single MSC transplantation. Two specialists analyzed CT scanning results, including lung shadows and honeycomb-like shadows.

Blood routine examination and blood gas analysis

At different time points, the dogs were anaesthetized to obtain femoral venous blood. White blood cell counts (WBC) and lymphocyte percentages were measured with a hemocytometer (Countess automated cell counter, Invitrogen, Paisley, UK). Femoral arterial blood was also taken. For evaluation of pulmonary function, we used a blood gas analyzer (i-STAT Corporation, Windsor, NJ) to measure the blood oxygen partial pressure (PO_2), the blood carbon dioxide partial pressure (PCO_2), pH value, and bicarbonate (HCO_3^-) concentration.

Enzyme-linked immunosorbent assay

We used enzyme-linked immunosorbent assay kits (Sangon Biotech, Shanghai, China), per manufacturer's instructions, to measure serum levels of TGF-α, TGF-β, hydroxyproline, and hyaluronic acid (HA) as well as the lung tissue levels of HA, tumor necrosis factor-α (TNF-α), interleukin 1 (IL-1), superoxide dismutase (SOD) and malondialdehyde (MDA). Samples from the injured sites of the right lower lobe were homogenized in ice-cold phosphate-buffered saline. The homogenates were centrifuged at 1000 g for 10 minutes at 4°C. The supernatants were stored at −80°C until analysis. Protein concentration was determined using the BCA Protein Assay Kit (Beyotime, Haimen, Jiangsu, China). Enzyme-linked immunosorbent assay kits were species-specific. After the reaction was completed, the optical density values were measured at 450 nm with a microplate reader (Bio-rad 550, BioRad Laboratories). The experiment was repeated twice. The interassay coefficient of variation (%CV) of IL-1 was 7.0%, %CV of TNF-α was 4.6%, %CV of HA was 8.6%, %CV of TGF-α was 6.5%, %CV of TGF-β was 8.5%, %CV of hydroxyproline was 7.4%, %CV of SOD was 6.6%, and %CV of MDA was 9.5%.

Histological examination

Samples from the injured sites of the right lower lobe were embedded in paraffin and sectioned at a thickness of 5 μM. Samples from the injured sites were selected based on CT scanning results (Fig. E1; available online at www.redjournal.org). Hematoxylin and eosin staining and Masson staining were conducted to assess lung pathology. The images were collected with the Olympus BX5 microscope (Olympus, Tokyo, Japan) by 2 professionals who knew nothing about the study. In addition, the percentage of the area of positive collagen fibers (blue) to total area of cells was analyzed with Image-Pro Plus 6.0 software (Media Cybernetics, Bethesda, MD) on 5 randomly selected 40 high-power fields under light microscope.

Immunofluorescence staining

Lung tissue sections were stained using TGF-β1 primary antibody and Cy3-labelled secondary antibodies, as described in Materials E1 (available online at www.redjournal.org).

Alveolar epithelial cell II isolation and treatment

Primary alveolar epithelial cell II (AECII) isolation was conducted as previously described (24), and the methods of AECII isolation and collection of MSCs-conditioned medium (MSCs-CM) are described in Materials E1 (available online at www.redjournal.org). After 24 hours of incubation, AECII were treated with the collected MSCs-CM (100%) and/or TGF-β1 (5 ng/mL; Sigma, St Louis, MO) for 48 hours, whereas the control cells were released in the normal medium.

Western blot analysis

Protein samples were separated by sodium dodecyl sulfate polyacrylamide gel electrophoresis, and Western blots were done as previously described (25). Briefly, the proteins were separated and transferred to polyvinylidene fluoride membranes. After blocking with 5% nonfat milk, the membranes were incubated overnight at 4°C with polyclonal antibodies. Over the next days, proteins were visualized using the enhanced chemiluminescence detection system (Millipore, Saint-Quentin-en-Yvelynes,

France) after incubation with appropriate secondary antibody. The polyclonal antibodies against phospho-Smad2, phospho-Smad3, Smad2, Smad3, and TGF-β1 were all from Cell Signaling (Cell Signaling Technology, Beverly, MA). The band intensity was quantified by the LAS3000 apparatus (Fujifilm, Raytest, Courbevoie, France). β-actin was used as the internal control to verify equal protein loading.

Statistical analysis

SPSS13.0 statistical software (SPSS Inc, Chicago, IL) was used for statistical analysis, and the results were represented by mean ± standard deviation. Normality was evaluated by the Shapiro-Wilk test. The paired sample Student *t* test compared the differences between before and after radiation. The independent samples *t* test compared the means between saline and MSC treatments. For comparisons among multiple groups, statistical analyses were performed by 1-way analysis of variance and Tukey's honest significant difference test for multiple comparisons. $P < .05$ indicated significant difference (2 sides).

Results

Establishment and evaluation of a canine model of radiation-induced lung injury

Changes in WBC and lymphocyte percentages after radiation

After the 8 dogs received right lower lung local radiation at 15 Gy, they did not show significant declines in appetite, body weight increased steadily, body temperature was maintained at 37°C to 38°C, and heart rate was 85 to 105 beats per minute. The dogs showed no obvious signs of cough or hemoptysis. One of the dogs had a higher respiratory rate 1 week after radiation, which was maintained at approximately 32 beats per minute, and no other abnormalities were observed.

WBC fluctuated in the range of 6.6 to 10×10^9/L within 0 to 180 days after radiation, which was in the normal range of WBC for dogs. The proportions of lymphocytes before and after radiation did not change significantly (Fig. E2; available online at www.redjournal.org), which indicated that 15-Gy local radiation may not affect the systemic hematopoietic function.

Arterial blood gas analysis after radiation

To observe changes in the lung function of dogs after radiation, arterial blood gas analysis was performed at different time points (Fig. E3; available online at www.redjournal.org). The results showed that PO_2 decreased gradually, by approximately 50% on the 180th day. The changes in PCO_2, HCO_3^- concentration, and pH were small, and the values remained stable before and after radiation.

Changes in serum hydroxyproline and transforming growth factors after radiation

The serum hydroxyproline content increased gradually after radiation and reached approximately 30 ug/mL on the 180th day after radiation (Fig. 1A), which was significantly higher than the value observed before radiation. Similarly, the TGF-β level was also significantly increased on the 180th day after radiation, suggesting that the degree of fibrosis became more severe (Fig. 1C). In contrast, the TGF-α level showed a trend of decrease after radiation (Fig. 1B).

Evaluation of the therapeutic effect of MSCs on radiation-induced lung injury

Preparation and characterization of clinical-grade human umbilical cord MSCs

The flowchart (Fig. 2A) demonstrates the bioprocess of MSC preparation for clinical use, including cell isolation, expansion, and characterization as well as safety assessment before transplantation. Fibroblastic-shaped cells could be observed under microscope during the process of cell expansion (Fig. 2B). The human umbilical cord MSCs (hUC-MSCs) had normal karyotypes without mutations (Fig. 2C) and a high cell viability of 97%. Phenotypic analysis and differentiation experiments were carried out from passage (P) 3 to P10 (Figs. 2D and 2E). Flow cytometry analysis showed that purity of hUC-MSCs was over 99%, confirmed by high positive rates of CD105, CD73, CD90, and CD29 and negative expression of HLA-DR, CD34, CD45, CD14, CD40, CD80 and CD86 (Fig. 2D). Immunofluorescence staining results demonstrated specific expression of FABP, osteocalcin, and aggrecan (Fig. 2E), and MSCs show the capability of differentiating into adipocytes, osteoblasts, and chondrocytes. P5 hUC-MSC products were transported to the hospital for endotracheal administration. Safety assessment were carried out before cells were transplanted, including cell identification, fungal and bacterial test, mycoplasma testing, virus testing, and endotoxin and BSA tests (Table E1; available online at www.redjournal.org), which confirmed that MSCs were biologically safe.

Changes in lung imaging results after MSC transplantation

At 180 days after 15-Gy radiation, the right lung CT results revealed grid-like shadows, irregular thickening of the interlobular septum, significant thickening of the lobular small blood vessel wall, and honeycomb shadows in the right middle and lower pulmonary pleurae (Fig. 3). After treatment with MSCs, the results showed that the honeycomb shadow gradually decreased over time, which suggested that the degree of injury was gradually reduced. After saline treatment, the honeycomb shadow was significantly enlarged on the 30th day, but the shadow area also

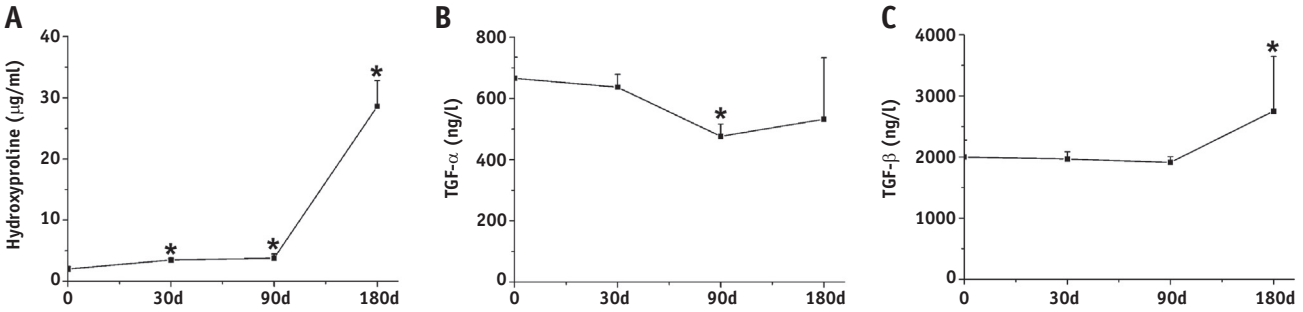

Fig. 1. Effects of radiation on serum hydroxyproline and transforming growth factors of dogs at different time points. The serum levels of hydroxyproline (A), transforming growth factor-α (TGF-α) (B), and TGF-β (C) were measured using enzyme linked immunosorbent assays (ELISA) kits according to the manufacturer's instructions. Data are expressed as mean ± standard deviation (n = 8) and analyzed by paired sample Student *t* test. $*P < .05$, compared with nonradiation group (corresponding to 0 day).

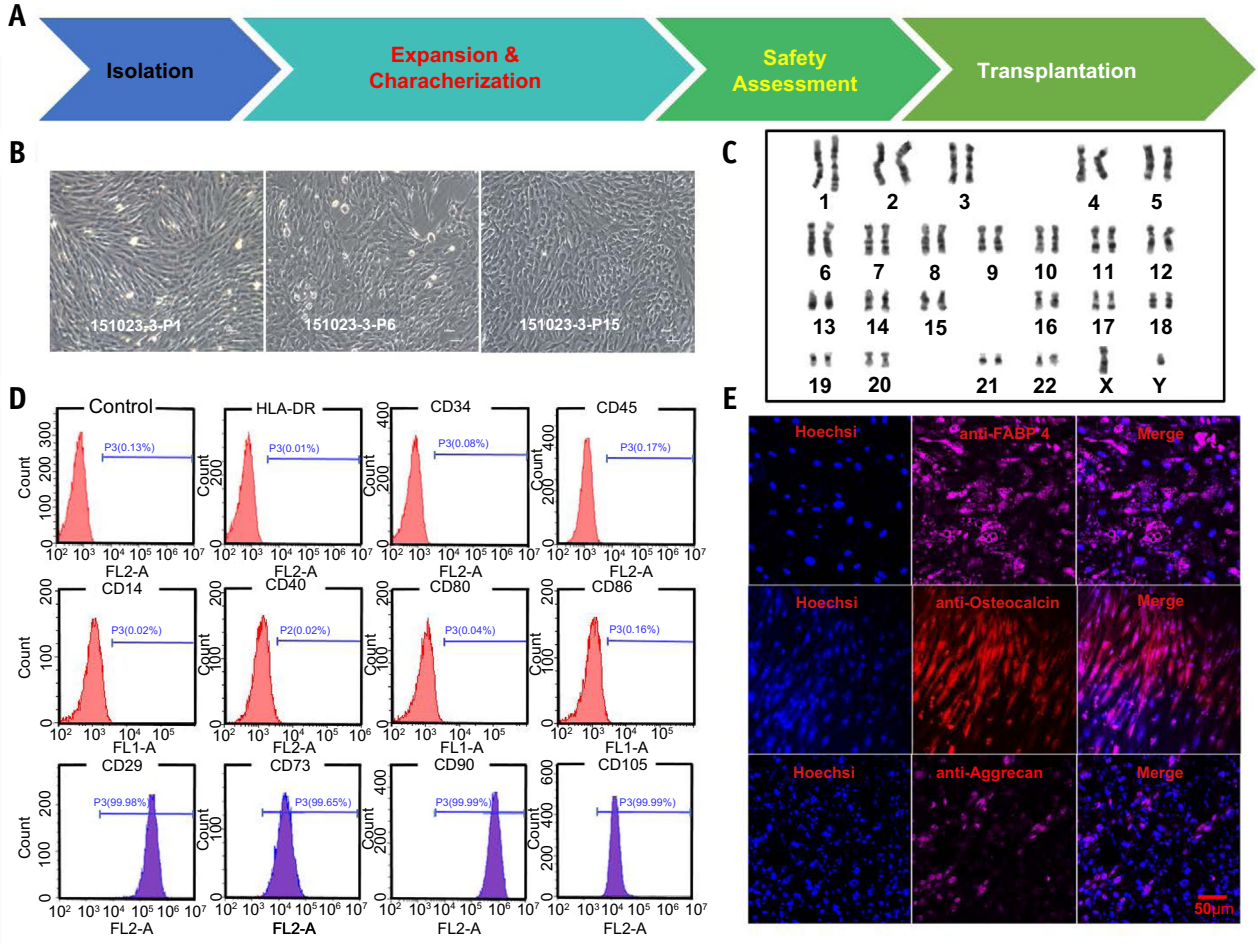

Fig. 2. Morphology and features of mesenchymal stem cells (MSCs). (A) The bioprocess of MSC preparation for clinical use. (B) The MSCs exhibited a spindle-like shape under in vitro culture. (C) The karyotype analysis of human umbilical cord mesenchymal stem cells (hUC-MSCs). (D) Quantitative analysis of MSCs by flow cytometry analysis. (E) Tri-lineage differentiation of MSCs. MSCs were fixed and probed with fatty-acid-binding protein, osteocalcin, and aggrecan antibody; nuclei were visualized by staining with Hoechst (blue). The image was visualized by using confocal microscopy. (A color version of this figure is available at www.redjournal.org.)

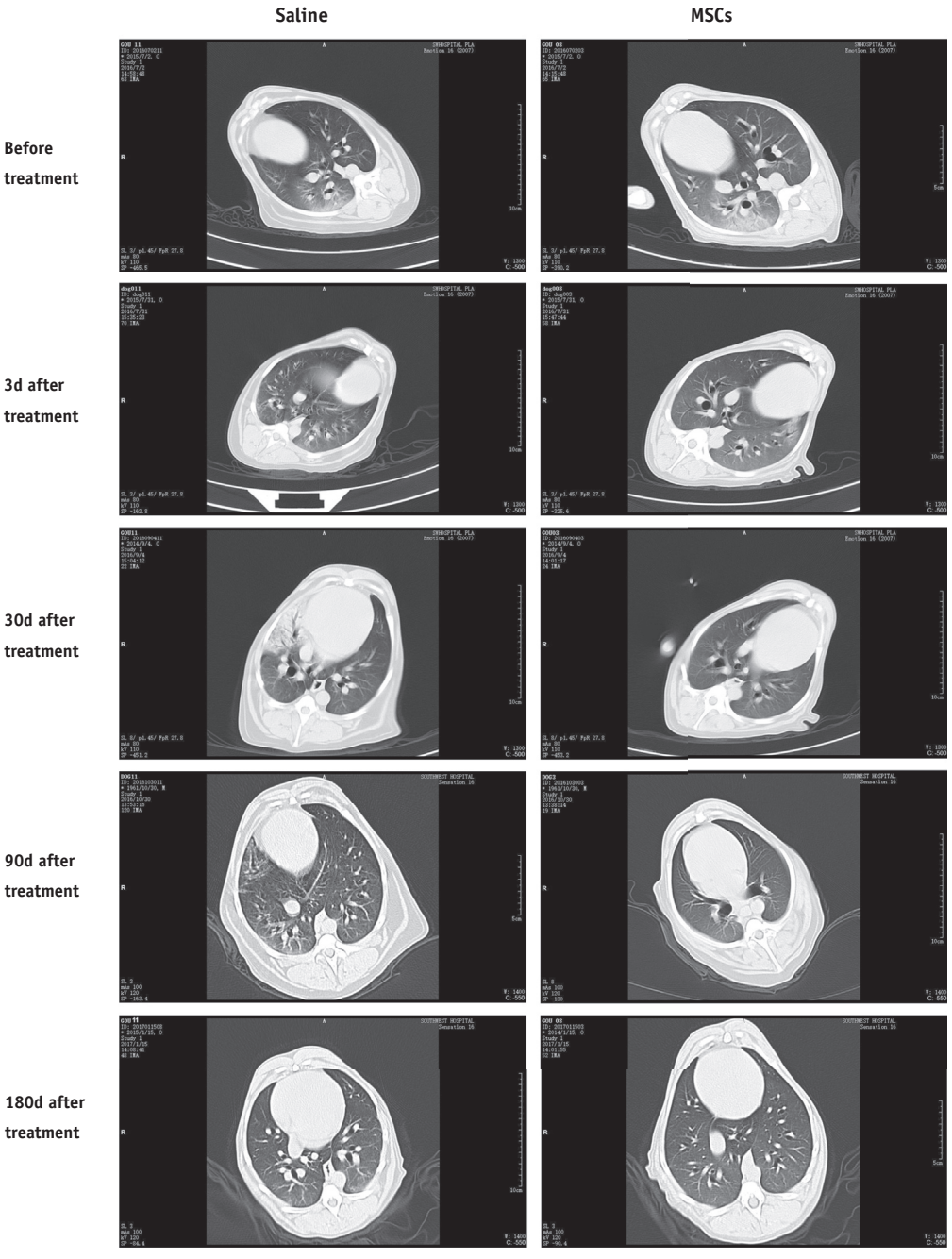

Fig. 3. Protective effects of mesenchymal stem cells (MSCs) on lung computed tomography images of dogs after radiation. The experimental dogs received MSC transplantation or normal saline lavage and underwent chest computed tomography under full anesthesia; we used a third generation computed tomography scanner at different time points.

gradually decreased over time, indicating that the degree of injury was reduced but remained more severe than that observed in the MSC group.

Changes in leukocyte and lymphocyte percentages after MSC transplantation

Dogs, whether treated with MSC transplantation or saline, showed no respiratory symptoms. WBC and lymphocyte percentages were not significantly affected in the saline treatment or the MSC groups. Within 180 days of treatment, WBC and lymphocyte percentages all fluctuated within normal ranges (Fig. E4; available online at www.redjournal.org).

Analysis of arterial blood gas after MSC transplantation

To evaluate the effect of MSC transplantation on the lung function of dogs after radiation, arterial blood gas analysis was performed at different time points (Fig. E5; available online at www.redjournal.org). The results showed that PO_2 gradually increased with time after MSC transplantation,

and the difference was significant compared with the saline group. These results also indicated that MSC transplantation could improve lung function. In contrast, the changes in PCO_2, HCO_3^- concentration, and pH value were small, and there were no significant differences when compared with the saline group.

Changes in lung pathology and fibrosis after MSC transplantation

At 180 days after transplantation, the saline group presented inflammatory cell infiltration accompanied by collagen formation, and the injury seemed more severe than that observed in the MSC group (Fig. 4A). Masson staining further revealed that the collagen level in the saline group was higher than that in the MSC group (Figs. 4B and 4C).

Changes in oxidative stress, inflammatory factors, HA, and serum TGF in lung tissue after MSC transplantation

Compared with the saline group, the SOD level was significantly higher, the MDA level lower, and the levels of TNF-α and IL-1 significantly lower in the injured lung tissue in the MSC group at 180 days after transplantation (Figs. 5A-5D). We also found that the levels of HA in serum and lung tissues at 180 days after MSC transplantation were significantly lower than those in the saline group (Figs. 5E and 5F). Within 180 days after MSC transplantation, serum hydroxyproline showed a downward trend (Fig. 5G) and differed significantly from the trend observed in the saline group. Similarly, the serum TGF-β was also significantly decreased after MSC transplantation, which suggested aggravated degrees of fibrosis (Fig. 5I). In contrast, serum TGF-α increased gradually after MSC transplantation (Fig. 5H).

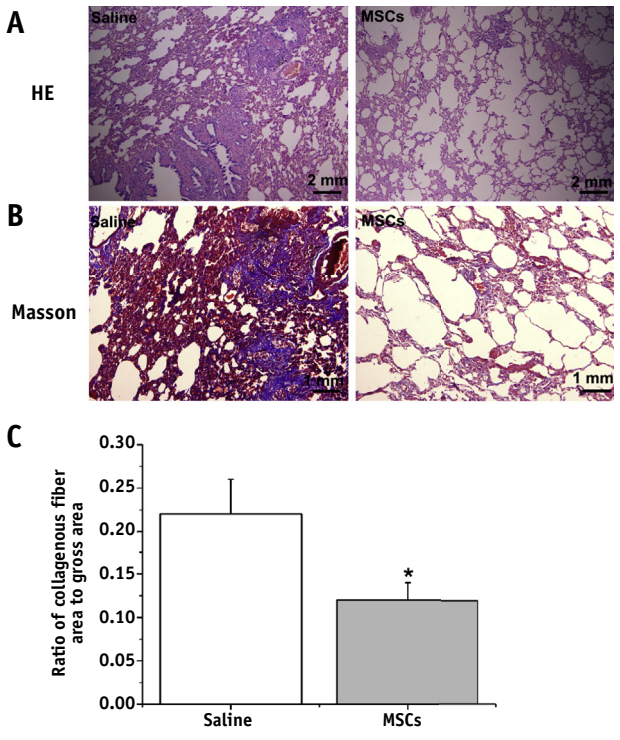

Fig. 4. Effects of mesenchymal stem cells (MSCs) on lung histologic changes and collagen deposition in dogs after radiation. (A) Hematoxylin and eosin staining of lung tissues in saline and MSC groups at 180 days after saline or MSC treatment. (B) Pulmonary tissue sections were subjected to Masson's staining for the visualization of collagen deposition (blue). (C) Histopathology fibrosis score was quantified with the proportion of collagen deposition (blue) for each group. Data are expressed as mean ± SD (n = 4) and analyzed by independent samples *t* test. $*P < .05$, compared with saline group. (A color version of this figure is available at www.redjournal.org.)

Effect of MSCs on the TGF-β and Smad 2 and 3 signaling pathway

Compared with the saline group, TGF-β levels in the injured lung tissue were significantly lower at 180 days after transplantation, as revealed by Western blot, and the corresponding phospho-Smad2 and phospho-Smad3 levels were also decreased (Figs. 6A and [B). Immunofluorescence staining showed that the TGF-β level in lung tissues after MSC transplantation was significantly lower than that in the saline group (Fig. 6C). To understand the detailed mechanism of MSC activity on the TGF-β—Smad2/3 signaling pathway, we isolated AECII, which is commonly used as a model of PF in vitro. The results demonstrated that MSCs-CM effectively inhibited the upregulation of phospho-Smad2 and phospho-Smad3 expression in AECII induced by TGF-β (Figs. 6D and 6E).

Discussion

An increasing number of studies has shown that MSCs can differentiate into bronchial epithelial cells, alveolar epithelial cells, and fibroblasts in the lungs and have protective effects on radiation-induced lung injury in rats or mice (11, 26). However, small-animal models typically use whole-body or whole-lung radiation, which may cause a series of reactions involving multiple organs, making it difficult to observe the dynamic changes in specific lung tissue areas within the same animal. In this study, we used dogs, which have a lung size close to that of humans, and observed the process of radiation-induced lung injury and the protective effects of MSCs after localized 15-Gy radiation to the right lower lung. Similar studies have also pointed out that dog models enable further exploration of the nature of radiation-induced lung injury (20). Humans and dogs have a portion of respiratory bronchiole between the terminal bronchiole and alveoli, whereas rodents have alveolar ducts interposed between the terminal bronchiole and the alveoli (27); therefore, this study selected dog as an animal model. Further study will focus on the dose effect curve in the radiation-induced lung injury in this model and the kinetics of the evolution of pulmonary injury.

The results of this study lay the foundation for the clinical application of MSCs in the treatment of lung

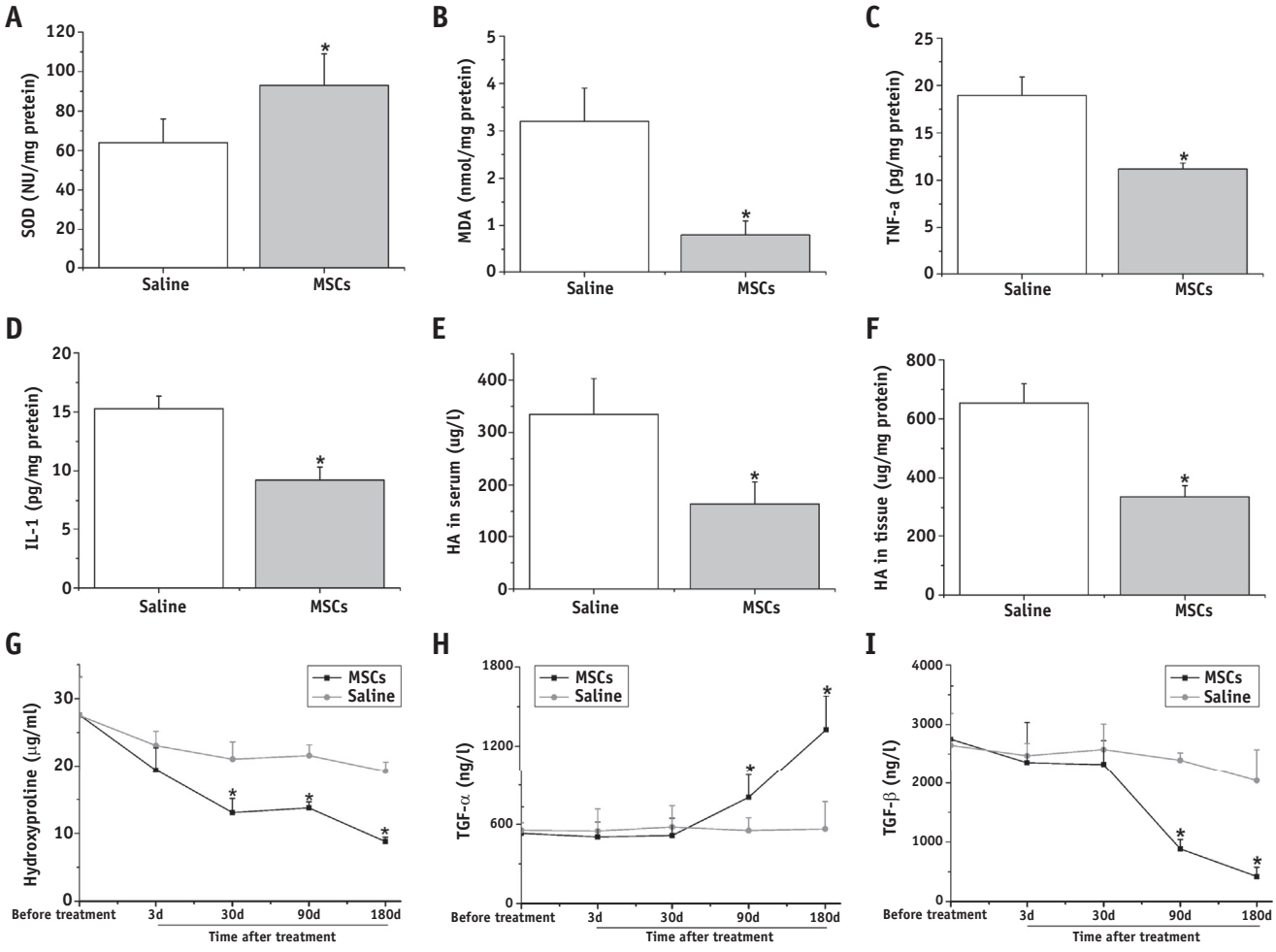

Fig. 5. Effects of mesenchymal stem cells (MSCs) on the levels of oxidative stress, inflammatory cytokines, and lung fibrosis after radiation. The superoxide dismutase (SOD) (A) and malondialdehyde (MDA) (B) contents in the lung tissue were detected using the corresponding kits as described in the Materials and Methods section. At 180 days after MSC transplantation, the serum levels of tumor necrosis factor-α (TNF-α) (C), interleukin 1 (IL-1) (D), hyaluronic acid (HA) (E), and the lung tissue levels of HA (F) were measured using enzyme-linked immunosorbent assay (ELISA) kits according to the manufacturer's instructions. The serum levels of hydroxyproline (G), transforming growth factor-α (TGF-α) (H), and TGF-β (I) were measured using ELISA kits according to the manufacturer's instructions at 3, 30, 90, and 180 days after MSC transplantation. Data are expressed as mean ± standard deviation (n = 4) and analyzed by independent samples Student *t* test. $*P < .05$, compared with saline group.

radiation injury. hUC-MSCs, often discarded as medical waste, are among the typical MSCs that offer the following advantages: elimination of invasive and uncomfortable extraction procedures; attractive immunologic properties for allogeneic transplantations because of low immunogenicity; ethical access compared with MSCs from other sources; and a substantial number of cells in several passages without need for long-term culture and extensive expansion ex vivo (28, 29). Therefore, the administration of hUC-MSCs might be considered a potential strategy for treatment of radiation-induced lung injury.

This study confirmed that MSC transplantation has a protective effect against radiation-induced lung injury in dogs. Kursova et al found that MSC transplantation reduced mortality in a mouse model of radiation-induced lung injury (30). In clinical applications, MSCs have been used in the treatment of diseases such as pneumonia and lung injury caused by sepsis and achieved satisfactory results (31, 32). Bone marrow−derived MSC transplantation delayed the lung injury deterioration process in 11 cases of thoracic radiation therapy−caused radiation PF, and long-term follow-up did not identify MSC-induced tumor development. The cell dose of MSCs for the treatment of chronic obstructive pulmonary disease is 100×10^6 cells per person (33), if the average body weight of patients is 80 kg and the dose is 1.25×10^6 MSC/kg. Similar studies have shown that the efficacy of a single-dose MSC lavage at 0.1×10^3/g is equivalent to that of MSC treatment at 1×10^5/kg (34). Tzouvelekis et al demonstrated that, after intratracheal transplantation of MSCs in 14 patients

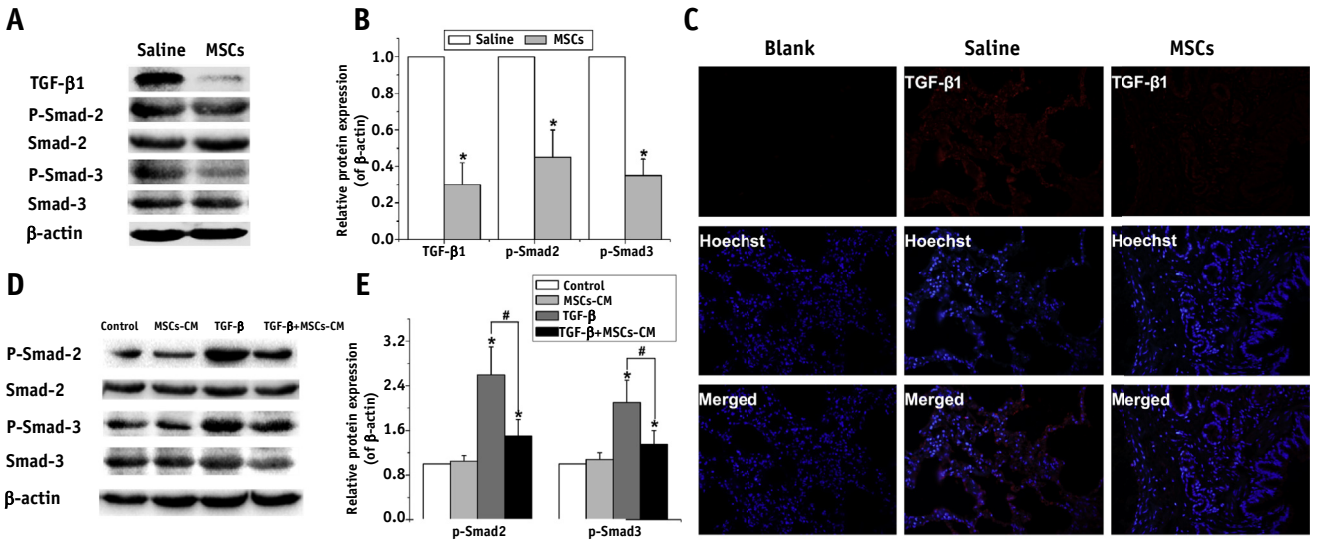

Fig. 6. Effects of mesenchymal stem cells (MSCs) on transforming growth factor (TGF)-β1−Smad2/3 signaling pathway. The protein expression levels of TGF-β1, Smad2/3, and phospho-Smad2/3 in lung tissues from the saline and MSC groups were analyzed by Western blot. (A) The representative bands are shown. (B) The density values of blots were normalized to the internal control β-actin. Data are expressed as mean ± standard deviation (SD) (n = 4) and analyzed by independent samples Student *t* test. $*P < .05$, compared with saline group. (C) Immunofluorescence staining was performed to detect TGF-β1 protein expression (red) in lung tissue sections from each group, and there was no sodium-glucose linked transporter primary antibody in the blank (negative control). Nuclei were visualized by staining with Hoechst. In addition, primary alveolar epithelial cell II (AECII) isolation was conducted, and AECII were treated with MSCs-conditioned medium (CM) and/or TGF-β1 (5ng/mL) for 48 hours. The control cells were cultured in the normal MSC medium. The protein expression levels of Smad2/3 and phospho-Smad2/3 in in AECII from each group were analyzed by Western blot. (D) The representative bands are shown. (E) The density values of blots were normalized to the internal control β-actin. Data are expressed as mean (± SD) (n = 3) and analyzed by 1-way analysis of variance. $*P < .05$, compared with control group; $^{\#}P < .05$, Tukey's honest significant difference test for multiple comparisons. (A color version of this figure is available at www.redjournal.org.)

with different degrees of idiopathic PF, no clinically significant adverse reactions occurred within 12 months (35). In this study, MSCs (1×10^6 cells/kg) were transplanted via bronchofiberscopy to facilitate the local colonization of stem cells. According to the literature (36), MSC characterization should be better conducted at earlier generation; thus, we chose P5-MSCs for the experiments.

MSC transplantation could increase the activity of SOD in lung tissues and decrease MDA levels. Similar to our results, other research has shown that MSCs can recover the expression of SOD1 and thereby prevent radiation-induced reduction of endothelial cells (17). MSCs with high expression of SOD can reduce radiation-induced pulmonary inflammatory responses and lung injury (37). Similarly, this study found that MSC transplantation can reduce TNF-α, IL-1, and HA levels in lung tissues. HA is associated with the progression of pulmonary inflammation and PF (38). Studies have shown that inhibition of HA is an important antifibrosis mechanism of extracellular SOD (39). HA plays an important role in the regulation of TGF-β−induced fibrosis (40). TGF-β is a key player in the initiation and progression of PF and is widely considered a potential therapeutic target. In this study, we found that at 180 days after 15-Gy local radiation, the level of serum TGF-β was significantly increased, whereas the TGF-β level in the serum and tissue was decreased by MSC transplantation, as was expression of phospho-Smad2 and phospho-Smad3 in lung tissues. It has been shown that TGF-β acts through the regulation of Smad-dependent pathways to cause changes in target gene transcription levels, thus leading to PF (41). In this study, we also found that MSCs-CM significantly reduced TGF-β1-induced increases in the levels of AECII phospho-Smad2 and phospho-Smad3. Therefore, the mechanism by which MSCs attenuated radiation-induced lung injury may be inhibition of the activation of the TGF-β−Smad2/3 pathway. Similar studies have used AECII to test the inhibitory effects of induced pluripotent stem cells on PF by the TGF-β−Smad pathway (42).

Conclusions

Intratracheal MSC transplantation can reduce oxidative stress, inflammatory reactions, HA level, and TGF-β−Smad2/3 pathway activation, thereby reducing lung injury. This study provides a new approach for guiding MSC-mediated clinical treatment of complications such as radiation-induced pneumonitis and PF caused by radiation therapy treatment of thoracic tumors. It also provides a

basis for the application of MSCs in clinical transplantation therapies.

References

1. Tsoutsou PG, Koukourakis MI. Radiation pneumonitis and fibrosis: Mechanisms underlying its pathogenesis and implications for future research. *Int J Radiat Oncol Biol Phys* 2006;66:1281-1293.
2. Graves PR, Siddiqui F, Anscher MS, et al. Radiation pulmonary toxicity: From mechanisms to management. *Semin Radiat Oncol* 2010;20:201-207.
3. Abugideiri M, Nanda RH, Butker C, et al. Factors influencing pulmonary toxicity in children undergoing allogeneic hematopoietic stem cell transplantation in the setting of total body radiation-based myeloablative conditioning. *Int J Radiat Oncol Biol Phys* 2016;94:349-359.
4. Chargari C, Riet F, Mazevet M, et al. Complications of thoracic radiotherapy. *Presse Med* 2013;42:e342-e351.
5. Movsas B, Raffin TA, Epstein AH, et al. Pulmonary radiation injury. *Chest* 1997;111:1061-1076.
6. Adegunsoye A, Strek ME. Therapeutic approach to adult fibrotic lung diseases. *Chest* 2016;150:1371-1386.
7. Wei L, Zhang J, Yang Z, et al. Extracellular superoxide dismutase increased the therapeutic potential of human mesenchymal stromal cells in radiation pulmonary fibrosis. *Cytotherapy* 2017;19:586-602.
8. Qin M, Chen W, Cui J, et al. Protective efficacy of inhaled quercetin for radiation pneumonitis. *Exp Ther Med* 2017;14:5773-5778.
9. Pan J, Li D, Xu Y, et al. Inhibition of Bcl-2/xl with ABT-263 selectively kills senescent type II pneumocytes and reverses persistent pulmonary fibrosis induced by ionizing radiation in mice. *Int J Radiat Oncol Biol Phys* 2017;99:353-361.
10. Kuroda Y, Kitada M, Wakao S, et al. Bone marrow mesenchymal cells: How do they contribute to tissue repair and are they really stem cells? *Arch Immunol Ther Exp (Warsz)* 2011;59:369-378.
11. Ortiz LA, Gambelli F, McBride C, et al. Mesenchymal stem cell engraftment in lung is enhanced in response to bleomycin exposure and ameliorates its fibrotic effects. *Proc Natl Acad Sci USA* 2003;100:8407-8411.
12. Rojas M, Xu J, Woods CR, et al. Bone marrow-derived mesenchymal stem cells in repair of the injured lung. *Am J Respir Cell Mol Biol* 2005;33:145-152.
13. Kumamoto M, Nishiwaki T, Matsuo N, et al. Minimally cultured bone marrow mesenchymal stem cells ameliorate fibrotic lung injury. *Eur Respir J* 2009;34:740-748.
14. Jiang X, Qu C, Chang P, et al. Intravenous delivery of adipose-derived mesenchymal stromal cells attenuates acute radiation-induced lung injury in rats. *Cytotherapy* 2015;17:560-570.
15. Yu SH, Liu LJ, Lv B, et al. Inhibition of bleomycin-induced pulmonary fibrosis by bone marrow-derived mesenchymal stem cells might be mediated by decreasing MMP9, TIMP-1, INF-γ and TGF-β. *Cell Biochem Funct* 2015;33:356-366.
16. Abumaree M, Al Jumah M, Pace RA, et al. Immunosuppressive properties of mesenchymal stem cells. *Stem Cell Rev* 2012;8:375-392.
17. Klein D, Steens J, Wiesemann A, et al. Mesenchymal stem cell therapy protects lungs from radiation-induced endothelial cell loss by restoring superoxide dismutase 1 expression. *Antioxid Redox Signal* 2017;26:563-582.
18. McNulty K, Janes SM. Stem cells and pulmonary fibrosis: Cause or cure? *Proc Am Thorac Soc* 2012;9:164-171.
19. Yao Y, Zheng Z, Song Q. Mesenchymal stem cells: A double-edged sword in radiation-induced lung injury. *Thorac Cancer* 2018;9:208-217.
20. Yin Z, Deng S, Liang Z, et al. Consecutive CT-guided core needle tissue biopsy of lung lesions in the same dog at different phases of radiation-induced lung injury. *J Radiat Res* 2016;57:499-504.
21. Li X, Tan J, Xiao Z, et al. Transplantation of hUC-MSCs seeded collagen scaffolds reduces scar formation and promotes functional recovery in canines with chronic spinal cord injury. *Sci Rep* 2017;7:43559.
22. Gu Q, Hao J, Hai T, et al. Efficient generation of mouse ESCs-like pig induced pluripotent stem cells. *Protein Cell* 2014;5:338-342.
23. Luan Y, Zhang ZH, Wei DE, et al. Effects of autologous bone marrow mononuclear cells implantation in canine model of pulmonary hypertension. *Circ J* 2012;76:977-985.
24. Mutze K, Vierkotten S, Milosevic J, et al. Enolase 1 (ENO1) and protein disulfide-isomerase associated 3 (PDIA3) regulate Wnt/β-catenin-driven trans-differentiation of murine alveolar epithelial cells. *Dis Model Mech* 2015;8:877-890.
25. Hao Y, Liu C, Huang J, et al. Ghrelin protects against depleted uranium-induced apoptosis of MC3T3-E1 cells through oxidative stress-mediated p38-mitogen-activated protein kinase pathway. *Toxicol Appl Pharmacol* 2016;290:116-125.
26. Yan X, Liu Y, Han Q, et al. Injured microenvironment directly guides the differentiation of engrafted FLK-1(+) mesenchymal stem cell in lung. *Exp Hematol* 2007;35:1466-1475.
27. Peake JL, Pinkerton KE. Gross and subgross anatomy of lungs, pleura, connective tissue septa, distal airways, and structural units. Parent RA, editor. Comparative Biology of the Normal Lung. 2nd ed. London: Academic Press; 2015. p. 21.
28. Fan CG, Zhang QJ, Zhou JR. Therapeutic potentials of mesenchymal stem cells derived from human umbilical cord. *Stem Cell Rev* 2011;7:195-207.
29. Li T, Xia M, Gao Y, et al. Human umbilical cord mesenchymal stem cells: An overview of their potential in cell-based therapy. *Expert Opiniol Ther* 2015;15:1293-1306.
30. Kursova LV, Konoplyannikov AG, Pasov VV, et al. Possibilities for the use of autologous mesenchymal stem cells in the therapy of radiation-induced lung injuries. *Bull Exp Biol Med* 2009;147:542-546.
31. Qiao SK, Ren HY, Shi YJ, et al. Allogeneic compact bone-derived mesenchymal stem cell transplantation attenuates the severity of idiopathic pneumonia syndrome in a murine bone marrow transplantation model. *Cell Physiol Biochem* 2016;40:1656-1669.
32. Sammour I, Somashekar S, Huang J, et al. The effect of gender on mesenchymal stem cell (MSC) efficacy in neonatal hyperoxia-induced lung injury. *PLoS One* 2016;11:e0164269.
33. Weiss DJ, Casaburi R, Flannery R, et al. A placebo-controlled, randomized trial of mesenchymal stem cells in COPD. *Chest* 2013;143:1590-1598.
34. Kennelly H, Mahon BP, English K. Human mesenchymal stromal cells exert HGF dependent cytoprotective effects in a human relevant preclinical model of COPD. *Sci Rep* 2016;6:38207.
35. Tzouvelekis A, Bouros D. Steep barriers to overcome for successful application of stem cell treatment in patients with idiopathic pulmonary fibrosis. *Am J Respir Crit Care Med* 2013;188:251-252.
36. Keating A. Mesenchymal stromal cells: New directions. *Cell Stem Cell* 2012;10:709-716.
37. Chen HX, Xiang H, Xu WH, et al. Manganese superoxide dismutase gene-modified mesenchymal stem cells attenuate acute radiation-induced lung injury. *Hum Gene Ther* 2017;28:523-532.
38. Li Y, Jiang D, Liang J, et al. Severe lung fibrosis requires an invasive fibroblast phenotype regulated by hyaluronan and CD44. *J Exp Med* 2011;208:1459-1471.
39. Gao F, Koenitzer JR, Tobolewski JM, et al. Extracellular superoxide dismutase inhibits inflammation by preventing oxidative fragmentation of hyaluronan. *J Biol Chem* 2008;283:6058-6066.
40. Midgley AC, Rogers M, Hallett MB, et al. Transforming growth factor-β1 (TGF-β1)-stimulated fibroblast to myofibroblast differentiation is mediated by hyaluronan (HA)-facilitated epidermal growth factor receptor (EGRF) and CD44 co-localization in lipid rafts. *J Biol Chem* 2013;288:14824-14838.
41. Willis BC, Borok Z. TGF-beta-induced EMT: Mechanisms and implications for fibrotic lung disease. *Am J Physiol Lung Cell Mol Physiol* 2007;293:L525-L534.
42. Zhou Y, He Z, Gao Y, et al. Induced pluripotent stem cells inhibit bleomycin-induced pulmonary fibrosis in mice through suppressing TGF-β1/Smad-mediated epithelial to mesenchymal transition. *Front Pharmacol* 2016;7:430.

Erratum to: Hao Y, Ran Y, Lu B, et al. Therapeutic Effects of Human Umbilical Cord—derived Mesenchymal Stem Cells on Canine Radiation-Induced Lung Injury. *Int J Radiat Oncol Biol Phys* 2018;102:407-416.

In the original paper, there was an error in the part of "Reprint requests to". The corrected expression shall appear as below.

Reprint requests to: Jie Hao, PhD, Institute of Animals, Chinese Academy of Sciences, No. 1 Beichen West Road, Chaoyang District, Beijing, 100101, China, Tel.: +86 10 62558737, E-mail address: haojie@ioz.ac.cn; Rong Li, PhD, State Key Laboratory of Trauma, Burns and Combined Injury, Institute of Combined Injury, Chongqing Engineering Research Center for Nanomedicine, College of Preventive Medicine, Third Military Medical University, No.30 Gaotanyan Street, Shapingba District, Chongqing, 400038, China, Tel.: +86 23 68752281; E-mail address: yuhui_hao@126.com; Jianwu Dai, PhD, State Key Laboratory of Molecular Developmental Biology, Institute of Genetics and Developmental Biology, Chinese Academy of Sciences, Haidian District, Beijing, 100190, China, Tel.: +86 10 82614426, Email address: jwdai@genetics.ac.cn.

https://doi.org/10.1016/j.ijrobp.2018.10.012

DOI of original article: https://doi.org/10.1016/j.ijrobp.2018.05.068.